



Internal Short Circuit Trigger Method for Lithium-Ion Battery Based on Shape Memory Alloy

Mingxuan Zhang,^{a,b} Jiuyu Du,^a Lishuo Liu,^a Anna Stefanopoulou,^{b,*} Jason Siegel,^b Languang Lu,^a Xiangming He,^c Xiaoyi Xie,^c and Minggao Ouyang^{a,z}

^aState Key Laboratory of Automotive Safety and Energy, Tsinghua University, Beijing 100084, People's Republic of China

^bCollege of Engineering, University of Michigan, Ann Arbor, Michigan 48109, USA

^cInstitute of Nuclear and New Energy Technology, Tsinghua University, Beijing 100084, People's Republic of China

Internal short circuit (ISCr) is one of the major safety issues of lithium batteries and would lead to thermal runaway of batteries. Repeating ISCr in laboratory requires to create small-scale short circuit inside integrated batteries, which is very hard for existed safety test methods. In this paper, a novel ISCr trigger method based on shape memory effect of shape memory alloy (SMA) is proposed, which is easy to be implanted into batteries while has minor influences on batteries normal performance. The proposed SMA ISCr trigger method is employed to conduct ISCr experiments, including the severest type of ISCr, the Aluminum-Anode ISCr, and the most common type of ISCr, the Cathode-Anode ISCr. The experiments results show that the Aluminum-Anode ISCr leads to explosion while the Cathode-Anode ISCr only leads to mild self-discharging. Compared with the nail penetration test, the proposed SMA ISCr trigger method in the Aluminum-Anode ISCr experiment has 1) better consistency, given that all of the 4 tested batteries have their maximum temperature in the range of 383~393°C; 2) better reliability in evaluating battery safety properties, given that all of the 4 tested batteries have the repeatable explosion behavior. The relative ease of inserting this controllable SMA ISCr and the repeatability of the produced data can lead to better modeling and detection techniques of battery internal shorts such as plating and dendrite formation.

© The Author(s) 2017. Published by ECS. This is an open access article distributed under the terms of the Creative Commons Attribution Non-Commercial No Derivatives 4.0 License (CC BY-NC-ND, <http://creativecommons.org/licenses/by-nc-nd/4.0/>), which permits non-commercial reuse, distribution, and reproduction in any medium, provided the original work is not changed in any way and is properly cited. For permission for commercial reuse, please email: oa@electrochem.org. [DOI: 10.1149/2.0731713jes] All rights reserved.



Manuscript submitted August 28, 2017; revised manuscript received September 27, 2017. Published October 6, 2017. This was Paper 285 presented at the New Orleans, Louisiana, Meeting of the Society, May 28–June 1, 2017.

The lithium battery becomes more and more popular among electronic devices and electric vehicles, due to its high energy density, good power density and long cycle life.^{1,2} However, the intrinsic safety issues of energy storage devices haunt both of the development and application of lithium battery. Internal Short Circuit (ISCr) is one of the major safety hazards of lithium battery, which could lead to safety accidents like thermal runaway and result in catastrophic consequence.

The typical lithium-ion battery has two major parts, the positive part and the negative part, which are connected to positive terminal and negative terminal respectively (Figure 1a). The positive part consists of positive current collector (aluminum) and the porous positive electrode (cathode), the negative part consists of negative current collector and the porous negative electrode (anode). The two parts are separated by the porous separator, which allows ion transport but is electron insulating.³ The pores inside cathode, anode and separator are filled by the electrolyte, which allows ion transportation between the cathode and anode.

A controllable ISCr initiates electron conduction between the positive part and the negative part inside battery. Two positive components and two negative components can produce four types of ISCr, which are Cathode-Anode, Cathode-Copper, Aluminum-Anode, Aluminum-Copper (Figure 1b). The research of S. Santhanagopalan et al. in Ref. 4 shows that the Aluminum-Copper ISCr is the most severe one among the four types of ISCr due to both of its low ISCr resistance and mediocre heat dissipation. The Cathode-Anode ISCr is, however the most common type of ISCr, because it emerges once there are defects or tearing on the separator, while other types of ISCr still require further compromise of the battery structural integrity.

There are three types of conditions that could lead to ISCr, which are mechanical abuse, thermal abuse and self-induced. In the mechanical abuse case, the battery structure is compromised and the separator is torn by deformation.⁵ In the thermal abuse case, the separator collapses due to the high temperature.⁶ In the self-induced case, the separator is penetrated by dendrite or impurity given no external

trigger or reason.⁷ Compared with the mechanical abuse ISCr and the thermal abuse ISCr, the self-induced ISCr happens without crushing or other unusual external factors. The unnoticeable behavior of the self-induced ISCr increases its danger extent in field applications. In literature, the phrase Internal Short Circuit usually refers to the self-induced ISCr.

The practical ISCr happens rarely and it is hard to be repeated in laboratory. The broadly used safety tests method which emulate the abuse condition of batteries, such as crush, nail penetration, oven heating, etc., have twofold shortcomings of random results and external factors, and are not reliable for ISCr research and validation.⁸

Therefore, a controllable and repeatable ISCr experimental method is required to conduct research on battery ISCr. According to literature review, all the existed ISCr trigger methods have the same logic. One way to initiate ISCr is by pinching the battery until part of the separator are broken without penetrating the battery, including NASA round rod crush test,⁹ UL blunt nail test,^{10–12} ORNL-Motorola automated pinch test.¹³ These methods who attempt to initiate ISCr inside finished batteries do create short circuit. However, they distort the integrity of batteries, create short circuit in uncertain layers, transport heat and current to the battery shells and pinch rods,² and cannot control the type of ISCr. Another way to initiate ISCr is through implanting special triggers into batteries or through modifying batteries' structure. SNL developed an ISCr trigger method by fabricating cells with Ni particle contamination and triggering ISCr through media like sonication, thermal ramp and overcharge; they also used Sn/Bi/In alloy foil as potential short-inducing defect and initiate ISCr by heating.^{14–16} TIAX LLC suggested to implant metallic particles into the jelly-roll of batteries and initiating ISCr by repeated charge/discharge cycling.¹⁷ These ISCr trigger methods which involve metallic particles contamination may meet reliability and reproducibility challenges,¹⁸ and cannot control ISCr type. NREL developed an on-demand activation device to trigger different types of ISCr.^{18,19} A hole is cut on the separator and covered by Phase Change Material (PCM) trigger, the PCM trigger melts down above its' melting temperature and leads to ISCr of battery. This method is reliable on initiating different types ISCr, but it is difficult to fabricate experimental batteries and the PCM trigger will introduce in extra energy changing by phase changing and

*Electrochemical Society Member.

^zE-mail: ouymg@tsinghua.edu.cn

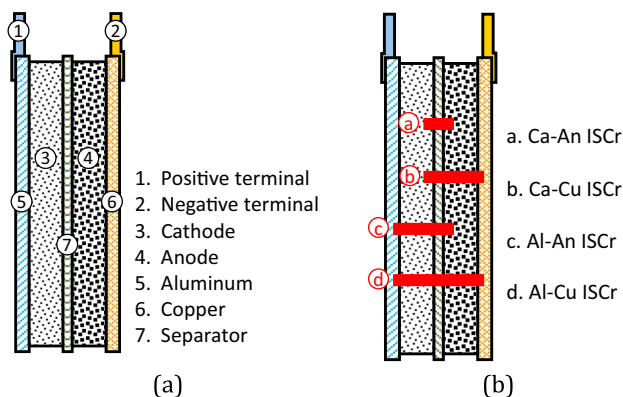


Figure 1. Schematic of lithium-ion battery structure and ISC. (a) Battery structure, the interstices inside cathode, anode and separator are fulfilled by electrolyte; (b) 4 types of ISC, Cathode-Anode, Cathode-Copper, Aluminum-Anode, Aluminum-Copper.

oxidization of PCM. Battery Association of Japan (BAJ) suggests to initiate ISC by placing a nickel particle into jelly-roll and trigger the ISC by compressing battery.²⁰ Celgard LLC presented an ISC trigger method by cutting a hole on separator to initiate ISC,^{8,21} an insulating film is positioned over the hole to avoid unexpected short circuit and removed during ISC initiation process. Both of the BAJ and Celgard methods requires disassembling and reassembling of fully charged batteries which is dangerous and difficult.

Shape memory alloy (SMA) could change its macroscopic shape as a response to its temperature change.²² This feature provides operators who use SMA the ability of reliable contactless control of mechanical motion: wireless, touchless, and even no integrated circuit. The SMA also has the advantage of compact size, high power/force density, corrosion-resistance, silence in action, and thus are applied in aerospace engineering, robotic engineering, biomedical engineering, etc.^{23–25} In this research, an ISC trigger method is proposed basing on SMA. The proposed SMA ISC trigger method could trigger different types of ISC and can be easily implanted into batteries. The batteries with proposed SMA ISC trigger almost have the same performance with normal batteries and can be charged/discharged as usual before initiation of ISC.

In Shape memory alloy battery internal short circuit trigger section, the background of SMA and the SMA ISC trigger are introduced. In Experimental battery fabrication section, the fabrication process of batteries with SMA ISC triggers is presented, and then the performance tests on batteries with the triggers are conducted. In ISC Experimental using SMA ISC Trigger section, experiments on the most severe ISC type, the Aluminum-Anode ISC, and the most common ISC type, the Cathode-Anode ISC, are conducted. The comparison of nail penetration tests is provided. Finally, the summaries and conclusions of the proposed SMA ISC trigger method are presented in Conclusions section.

Shape Memory Alloy Battery Internal Short Circuit Trigger

Shape memory alloy.—For SMA, it has two crystalline phase: austenite phase at high temperature and martensite phase at low temperature. The shape memory effect origins from the phase change of the SMA, namely thermoelastic martensitic transformation. Once martensite formed, it will grow from austenite along with the temperature decline. If temperature rises, martensite will decrease and transform into austenite conversely. As long as the deformation in martensite doesn't generate destruction of crystal lattice, the original array of the atoms of austenite could be remembered. When temperature rises, martensite changes into austenite which has the original array of atoms. At the same time, in macro scale, the SMA recovers to its preset shape of high temperature. This is known as shape memory effect, by which the SMA will recover to its preset shape once heated

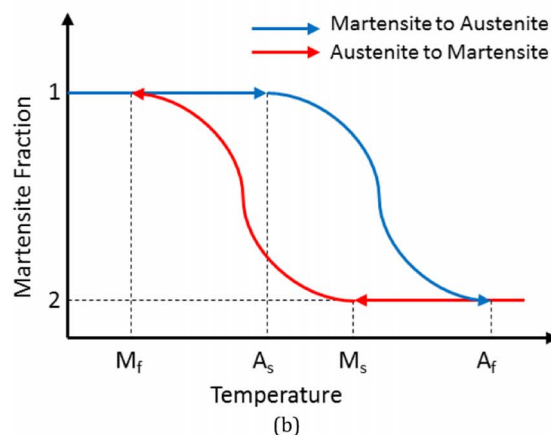
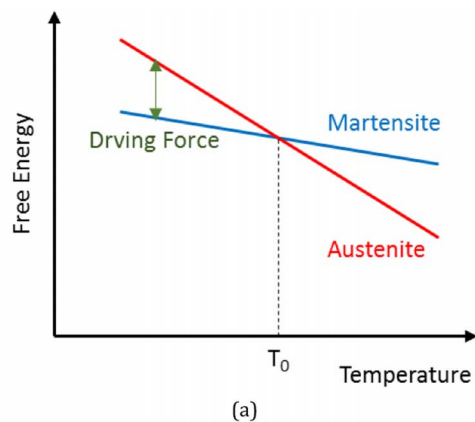


Figure 2. (a) – The driving force of thermoelastic martensite transformation; (b) – Diagram of the transformation between martensite and austenite.

above a certain temperature. The preset shape of SMA can be set by using heat-treatment.

The driving force of thermoelastic martensitic transformation, which behaves as shape recovery force in macro scale, is the difference between free energy of the two phases, Figure 2a. In equilibrium temperature, T_0 , the free energy of the two phases is equal, neither martensite nor austenite will change into the other phase. In temperature below T_0 , the free energy of austenite is higher than martensite, and the free energy difference pushes austenite change into martensite. In temperature above T_0 , the free energy of martensite is higher than austenite, and the free energy difference pushes martensite change into austenite.

However, there are also resistance against thermoelastic martensitic transformation, which results in that phase changing doesn't start exactly at T_0 . Martensite formation begins at temperature M_s and ends at temperature M_f , austenite formation begins at temperature A_s and ends at temperature A_f . This is shown in Figure 2b.

Shape memory alloy ISC trigger.—Using the shape memory effect of SMA, a new ISC trigger method could be invented. As elucidated before, the ISC is the internal electron conduction between the positive part and the negative part of batteries, which could be implemented by breaking the separator inserted between the positive part and the negative part. The shape memory effect gives SMA the ability to break the separator to trigger ISC inside battery by temperature control without destruction of battery integrity.

The SMA ISC trigger has the shape presented in Figure 3a, which mainly consists of two parts, the middle arrow and the two rectangle sides. The middle arrow is used to puncture separator and trigger ISC while the two rectangle sides are used to support the trigger itself. In low temperature, the SMA ISC trigger component will keep

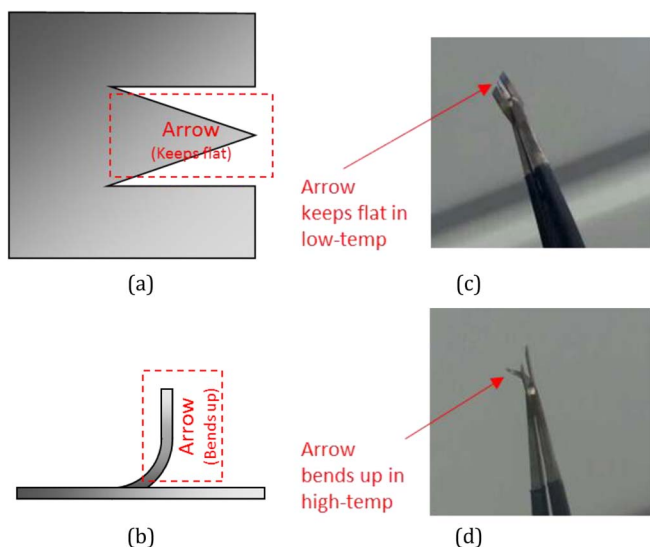


Figure 3. SMA ISCr trigger (a) – Sketch, plan view, flat shape in low temperature; (b) – Sketch, lateral view, arrow bends up in high temperature; (c) – Real trigger held with tweezers, flat shape in low temperature; (d) – Real trigger held with tweezers, arrow bends up in high temperature.

its flat shape, thus the arrow will not function. Once reaching high temperature, the arrow will bend up to its preset shape, as shown in Figures 3b, 3d, and further attempt to puncture the separator to trigger ISCr. The two rectangle sides will keep flat to provide support to the mid arrow. The preset shape of the SMA ISCr trigger is set by using heat-treatment. In this research, the SMA material is Ni-Ti alloy (Ni –50.85at%, Ti –49.10at%, other –0.05at%), the delivery A_f of the SMA material is $40 \pm 3^\circ\text{C}$, and the heat-treatment is $400\sim 500^\circ\text{C}$ heat preservation. However, after the heat-treatment and given there is additional resistance from battery structure press which requires more free energy to generate the driving force, the A_f of the SMA ISCr trigger is shifted to around 70°C .

Because of the SMA's advantage of compact size, high power/force density and corrosion-resistance,²³⁻²⁵ the SMA ISCr trigger won't influence the electrochemical system inside battery and can output sufficient executive power once reach its A_f temperature. Besides, in this research, the SMA ISCr trigger only has an area less than 1 cm^2 ($7.5\text{ mm} \times 7.5\text{ mm}$), which is very small compared with the area of entire jelly-roll. The thickness of it is 0.2 mm and can be easily implanted into jelly-roll. Therefore, the SMA ISCr trigger component have little influence on battery entire performance, and the battery can work normally before triggering ISCr. This will be proved by performance tests in Experimental battery fabrication section.

The SMA ISCr trigger component is placed aside the separator of battery in low temperature (flat shape), and the mid arrow's preset bending direction is toward the separator. Once the battery with the SMA ISCr trigger component inside is heated up, the SMA ISCr trigger component will be initiated and the mid arrow will puncture the separator. Then the battery ISCr happens.

The presented shape and deformation temperature of SMA ISCr trigger in this research is not the only choice. The principle to design SMA ISCr trigger is to have both of puncture arrow and support structure while keep the dimension as small as possible to reduce the influence on battery performance. The A_f temperature could be controlled by changing the ingredient ratio of SMA or employing certain heat-treatment process, which could be found in general literature of SMA.

Experimental Battery Fabrication

In this research, the 1Ah NCM lithium-ion pouch batteries fabricated by Jiangsu Huadong Institute of Li-ion Battery are used as

Table I. The Information of the Experiment Batteries.

Parameter	Value	Unit
Cathode	NCM	-
Type	Prismatic Pouch	-
$L \times W \times H$	$60 \times 50 \times 4$	mm
Cell	Jelly-Roll (Wound)	-
Capacity	1	Ah
Thickness of Cathode	92	μm
Thickness of Anode	98	μm
Thickness of Separator	17	μm
Thickness of Current Collector (+)	15	μm
Thickness of Current Collector (-)	10	μm

research object. The information of this type battery is listed in Table I.

Battery fabrication process.—To fabricate the batteries for ISCr experiments, battery jelly roll should be fabricated first. Hot compressing on jelly roll is suggested to acquire high compaction density. And jelly roll is baked in vacuum drying oven to dehumidify. Then place the SMA ISCr Trigger into the jelly roll inside glove box (Figure 4) and half-seal the battery using laminated aluminum film. After adding electrolyte into the battery, remove air content through vacuum cabin and then full-seal the battery. Wait until the electrolyte infiltrate the jelly roll. Finally, activate the cell and cut off the air bag of the laminated aluminum shell. Conduct capacity test or resistance test to check the performance of batteries with the SMA ISCr triggers.

Overall, the fabrication process of the batteries with the SMA ISCr triggers only has few differences with the normal batteries. Therefore, it's very convenient to implant the SMA ISCr triggers into batteries and initiated ISCr for researches and safety tests.

The quality of battery components and the completion of fabrication process, such as coating amount, compaction density, vacuum, etc., may significantly influence the battery performance and later behavior in experiments. Besides, the environmental condition in fabrication process, especially humidity, also has a great influence on battery performance. Therefore, for the fabrication of the batteries with the SMA ISCr triggers, the influence factors should be also carefully controlled as the well-designed procedure in normal battery manufacture.

Experimental batteries for different ISCr types.—The SMA ISCr trigger is placed adjacent to battery separator and the designated bend direction of the sharp arrow is pointing toward the separator.

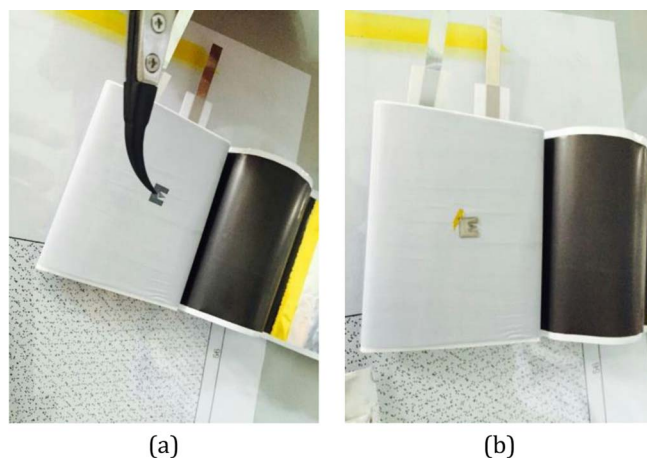


Figure 4. (a) – Put the SMA ISCr trigger into jelly-roll; (b) – The SMA ISCr trigger is positioned on the separator.

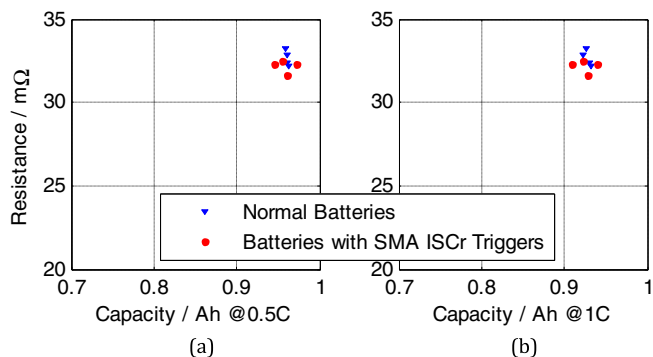


Figure 5. Capacity and resistance comparison between normal batteries and batteries with the SMA ISCr triggers. Resistance is measured at 50% SOC. (a) – Capacity is measured under 0.5C; (b) – Capacity is measured under 1C.

Therefore, after initiation of the SMA ISCr trigger, the sharp arrow will puncture the battery separator and lead to battery ISCr.

Without any additional modification to the jelly-roll, the ISCr experiments on batteries with the SMA ISCr trigger will result in the Cathode-Anode ISCr, because the SMA ISCr trigger will connect the cathode and anode on the two side of separator after initiation. With the removal of small area of certain activate material layer adjacent to the SMA ISCr trigger, other types of ISCr can be triggered using the SMA ISCr trigger: remove positive active materials to acquire the Aluminum-Anode ISCr; remove negative active materials to acquire the Cathode-Copper ISCr; remove both positive and negative active materials to acquire the Aluminum-Copper ISCr.

Performance tests for batteries with SMA ISCr triggers.—Capacity tests and resistance tests are conducted for both normal batteries and batteries with the SMA ISCr triggers. Figure 5 shows the capacity tests and resistance tests results. No obvious difference can be identified between normal batteries and batteries with the SMA ISCr triggers. The 1 Ah capacity of the tested batteries is relatively small, even much smaller than the widely used 18650 batteries which normally have capacity of 2~3 Ah. Therefore, it can be expected that the SMA ISCr triggers will have no obvious influence either when applied in larger capacity batteries.

In this research, before every ISCr experiment, capacity tests and resistance tests are conducted for the experimental batteries to make sure the batteries are in good condition.

ISCr experimental using SMA ISCr trigger.—The most severe ISCr, the Aluminum-Anode ISCr, and the most common ISCr, the Cathode-Anode ISCr, are presented. The nail penetration test, which is employed in several certification legislations to test ISCr safety of batteries, is conducted for comparison.

The Aluminum-Anode ISCr experiment.—Batteries with the SMA ISCr triggers for the Aluminum-Anode ISCr are fabricated. The SMA ISCr triggers are positioned at the center of the batteries and a small portion of positive material adjacent to the SMA ISCr trigger is removed to expose partial of the aluminum current collector directly to the SMA ISCr trigger. The batteries are heated by oven to the A_T temperature of the SMA ISCr trigger (70°C) in order to have the SMA ISCr triggers deform to their preset shape and puncture the separator.

The Aluminum-Anode ISCr experiment is conducted on experimental batteries, Al-An1 and Al-An2. And a normal battery is used for comparison. All of them are placed inside a large controlled oven at the same time to provide better comparison. The temperature of the oven is increased gradually. Once battery ISCr occurs, which is judged by whether there is terminal voltage drop, the oven temperature will no longer be increased.

Figure 6 shows the terminal voltage curves and center surface temperature curves of the experiment. Both of Al-An1 and Al-An2

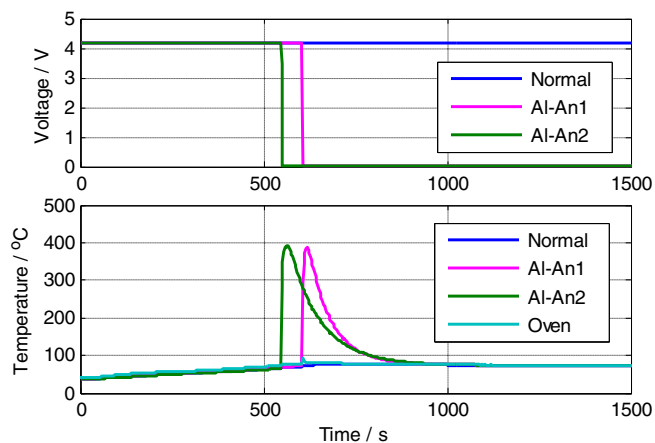


Figure 6. Terminal voltages and center surface temperatures of the Aluminum-Anode ISCr experiment. The normal battery is used for comparison.

have similar profiles. ISCr occurs around 70°C . The terminal voltages of batteries drop to 0V suddenly, and the pouch batteries explode with the center surface temperature reaching their maximum within minute. The sudden terminal voltage drop indicates small ISCr resistances and can be elucidated by the Parameter Effect of ISCr,²⁶ which refers to the phenomenon that the measured open circuit voltage (OCV) of ISCr battery is smaller than the real OCV due to the existence of short circuit loop. Fire, sparks and large amount of white smoke are witnessed. At the same time, the normal battery without the SMA ISCr trigger has a flat terminal voltage curve and a center surface temperature curve coincident with ambient. The results of the Al-An1 and Al-An2, as well as the results from other Aluminum-Anode ISCr experiment using the same method (Al-An3 and Al-An4) are listed in Table II. All of the 4 batteries get explosion shortly after the initiation of ISCr and output similar maximum temperature between 383°C and 393°C (a 10°C range).

The Aluminum-Anode ISCr experiment is also carried out in open field, in order to capture the pictures of explosion process. The battery with SMA ISCr triggers is fixed on iron set using clips. Hot wind gun is employed to generate the required temperature to initiate ISCr. Figure 7 shows the explosion scenario during the Aluminum-Anode ISCr process. First, the battery swells and erupts fire and some white smoke are visible at the center of the battery pouch, where the SMA ISCr trigger is implanted. Then, within seconds, the pouch's sealing edge with terminals burns down and erupts out burning materials. Finally, a large amount of white smoke is generated by the battery. Because of the influence of hot wind gun, the temperature measurement is not reliable in this case and not taken into consideration. It should be stressed that even for the batteries with small capacity of 1Ah, the Aluminum-Anode ISCr brings grave consequences, and thus operators must prepare carefully and take sufficient protective measures for this experiment.

The Cathode-Anode ISCr experiment.—Batteries with the SMA ISCr triggers for the Cathode-Anode ISCr are fabricated. The SMA ISCr triggers are positioned at the center of batteries. Two experimental batteries, Ca-An1 and Ca-An2, are individually heated by Accelerating Rate Calorimeter (ARC) to monitor small temperature change,

Table II. The Aluminum-Anode ISCr experiment results.

Battery	Al-An1	Al-An2	Al-An3	Al-An4
ISCr Start Temperature	72.3°C	64.7°C	57.9	64.2
Max Center Surface Temperature	387.6°C	392.7°C	383.9	385.8
Time to Max Temperature	15s	21s	15s	21s

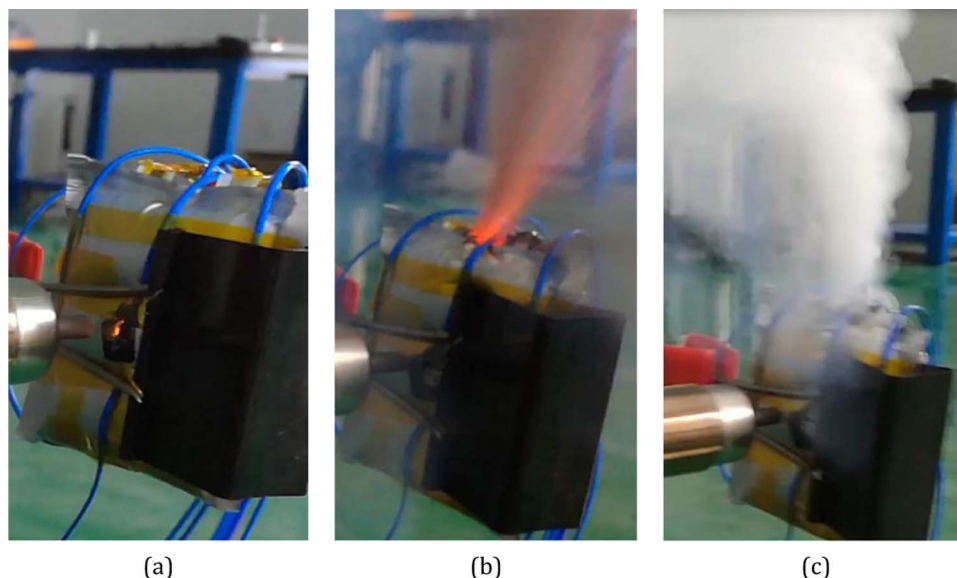


Figure 7. Aluminum-Anode ISCr experiment in open field. (a) – The battery swells and erupts at center of the pouch where the SMA ISCr trigger is implanted; (b) – The battery erupts out burning materials at the pouch's sealing edge with terminals; (c) The battery generate a lot of white smoke.

because the heat generation process of the Cathode-Anode ISCr is very mild. However, the heat generation scale of Cathode-Anode ISCr is even out of the accuracy of ARC in this research. Therefore, the temperature tracking mode of ARC cannot be achieved, neither the adiabatic condition. The heating process is stopped once reach the A_f temperature of the SMA ISCr trigger (70°C).

Figure 8 presents the terminal voltage curves and temperature curves of the Cathode-Anode ISCr experiment. The Ca-An1 and Ca-An2 have the similar profiles. The terminal voltages decrease in almost constant rates, and they never go to 0V as the Aluminum-Anode ISCr. The slow and continuous decline of terminal voltages indicates large ISCr resistance and can be explained by the Depleting Effect of ISCr,²⁶ which refers to the phenomenon that the real OCV of the ISCr battery

will decrease continuous due to the electrochemical energy depletion caused by short circuit. Because it's out of the ARC's accuracy to detect the heat generation of the Cathode-Anode ISCr, the adiabatic environment cannot be provided and the temperature of the batteries decline slowly from 70°C . It can be inferred from the terminal voltage curves, that battery Ca-An1 has relatively larger voltage decline than battery Ca-An2, which indicates larger heat generation from the Cathode-Anode ISCr. This is reflected on the slower temperature decreasing rate of battery Ca-An1. This difference is attributed to the short-circuit resistance difference. The Cathode-Anode ISCr has very high short resistance,⁴ therefore the short-circuit current depends on the short-circuit resistance instead of the battery internal resistance. The Cathode-Anode ISCr origins from the penetration of the SMA

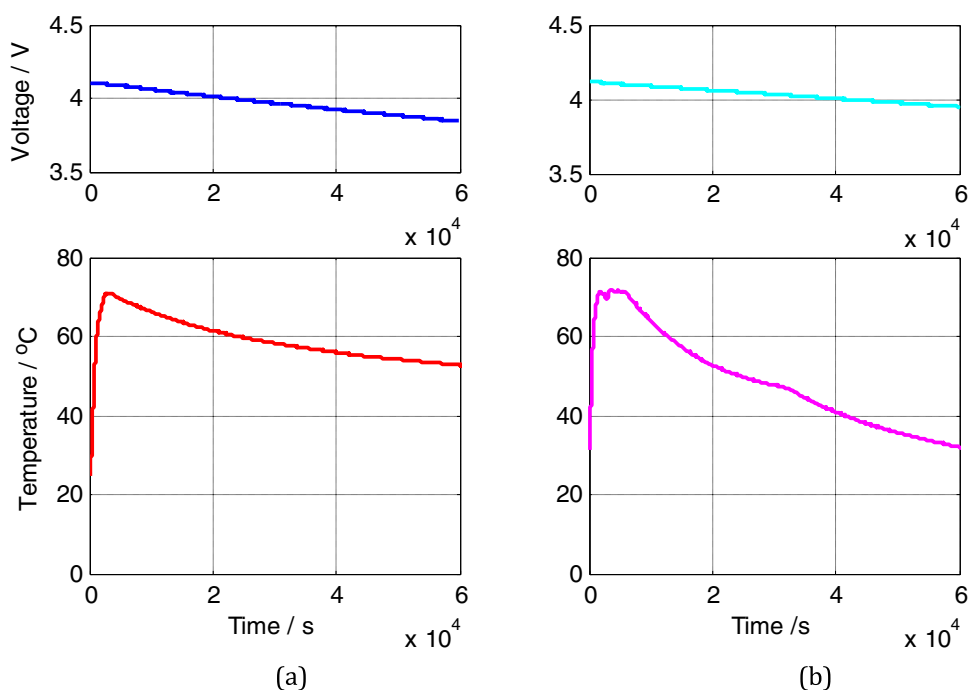


Figure 8. Terminal voltages and center surface temperatures of the Cathode-Anode ISCr experiment. (a) – Battery Ca-An1; (b) – Battery Ca-An2.



Figure 9. Disassembling result of the battery Ca-An1 after the experiment. Burnt traces can be found around the ISC area.

ISCr trigger and may have small resistance difference, which further results in difference in discharging rate. But for the Aluminum-Anode ISCr presented in foregoing section, which has very low short-circuit resistance,⁴ the short-circuit current mainly depends on the battery internal resistance. And small difference in short-circuit resistance has no obvious influence on the short-circuit current. Therefore, consistent results of the Aluminum-Anode ISCr can be expected.

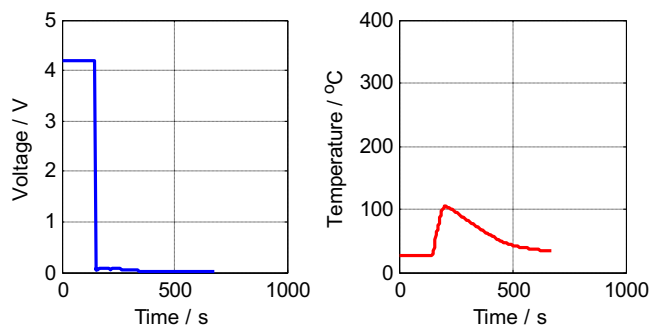
After the experiments, the exteriors of the Cathode-Anode ISCr experimental batteries are still intact. But burnt traces can be found in the area of jelly-roll where the SMA ISCr trigger is implanted after disassembling, as shown in Figure 9.

Comparison experiment using nail penetration.—Nail penetration test is conducted for comparison. A steel nail with diameter of 4 mm penetrates the batteries at the speed of 25 mm/s. Batteries are penetrated thoroughly at the center of pouch and the nail is kept inside the batteries after penetration. Three batteries, Nail1, Nail2 and Nail3, are tested. Figure 10 shows the curves of terminal voltage and temperature adjacent to the batteries center/penetration-spot. The experiment results are listed in Table III. Only one of the three tested batteries, Nail3, generates smoke and has a max temperature of 358.7°C, which is lower than the max temperature of the Aluminum-Anode ISCr experiment. No explosion or spark is witnessed for battery Nail3, which is possibly due to the pre-leakage caused by nail penetration. The other two batteries, Nail1 and Nail2, only have the max temperature around 105°C, which is much lower than the max temperature of Nail3 and the Aluminum-Anode ISCr experiment. It costs longer time to reach the max temperature for all of the nail penetration batteries than the Aluminum-Anode ISCr experiment. Generally, the nail penetration tests doesn't yield consistent results and may not reveal the worst scenario of ISCr, which means lack of reliability as concluded by P. Ramadass et al.⁸

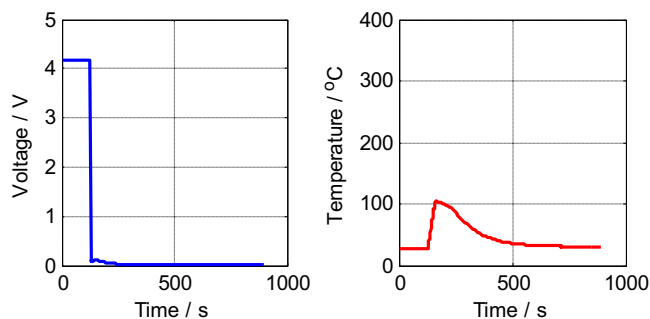
Compared with the nail penetration test, the proposed SMA ISCr trigger method in the Aluminum-Anode ISCr experiment yields better consistency and reproducibility, given that all of the 4 tested batteries have the maximum temperature within the range of 383~393°C. Furthermore, considering that one of the major aims of the safety test is to expose the worst case that could happen, the consistent explosion behavior of the Aluminum-Anode ISCr experiment indicates that the proposed SMA ISCr trigger method is more reliable in revealing the safety properties of batteries than the nail penetration test, which doesn't have explosion.

Conclusions

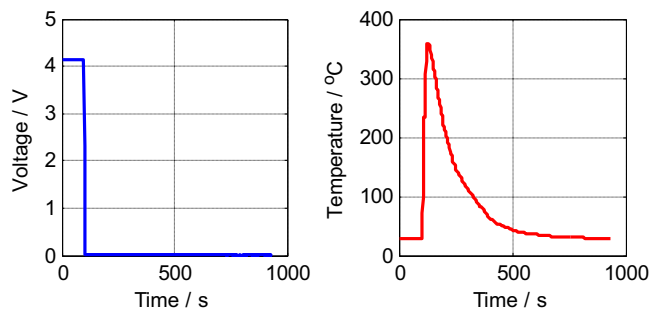
A novel ISCr trigger method based on the shape memory effect of SMA is introduced. The SMA ISCr trigger can be easily implanted



(a) Battery Nail1



(b) Battery Nail2



(c) Battery Nail3

Figure 10. Terminal voltages and temperature adjacent to penetration spots. (a) Battery Nail1; (b) Battery Nail2; (c) Battery Nail3.

into batteries during fabrication process and can trigger different types of ISCr while keeping the integrity of batteries. The size/area of the SMA ISCr trigger is very small compared with jelly-roll. Therefore, the SMA ISCr trigger has minor influence on battery performance, and the batteries with the SMA ISCr triggers can work normally before triggering ISCr. This is proved by performance tests. In this study, the SMA ISCr trigger has a deformation temperature, A_f , around 70°C, at which temperature it will recover to its preset shape and puncture battery separator, further initiate the battery ISCr.

The ISCr experiments are conducted for the most severe type of ISCr, the Aluminum-Anode ISCr, and the most common type of ISCr, the Cathode-Anode ISCr. For the Aluminum-Anode ISCr, the terminal voltage drops to 0V suddenly, and the center surface temperature climbs up rapidly and reach its maximum (383~393°C) within half minute. During the temperature increase process, the pouch battery

Table III. Nail penetration test results.

Battery	Nail1	Nail2	Nail3
Max Center Surface Temperature	104.2°C	105.6°C	358.7°C
Time to Max Temperature	56s	36s	31s

explodes and release a large amount of white smoke and fire, as well as, sparks are witnessed. For the Cathode-Anode ISCr, the terminal voltage declines gradually after the ISCr begins. The heat generation is too minor and out of the ARC's tracking capability used in this research. The pouch batteries' exterior stays intact after experiment, but burnt traces can be found in the ISCr areas in jelly-roll after disassembling the batteries. In summary, the Aluminum-Anode ISCr reacts rapidly and leads to grave consequences; the Cathode-Anode ISCr reacts slowly and mildly, it cannot individually lead to severe safety accidents.

Nail penetration tests are carried out for comparison. Three batteries are tested and all of them have terminal voltage dropping to 0V and temperature climbing up. However, only one of them has the max temperature of 358.7°C, while the others have the maximum temperature around 105°C, significantly lower than the Aluminum-Anode ISCr experiment. No explosion happens during nail penetration, neither fire nor spark is witnessed. And only the battery with the highest max temperature generates smoke while the others not. Generally, the nail penetration test doesn't yield consistent results for the same test, and its results are less severe than the Aluminum-Anode ISCr experiment and may not reveal the devastating consequence of ISCr.

In conclusion, the proposed SMA ISCr trigger method can trigger different types ISCr while keeping the integrity of batteries. The Aluminum-Anode ISCr experiment is able to reveal the most violent reaction of ISCr. The proposed SMA ISCr trigger method could be easily implemented during battery fabrication process. Compared with the traditional nail penetration test, the proposed SMA ISCr trigger method in the Aluminum-Anode ISCr experiment has: 1) better consistency and reproducibility, given that all of the 4 tested batteries in the Aluminum-Anode ISCr experiment has the maximum temperature within the range of 383~393°C while the nail penetration test has the maximum temperature of 104.2°C, 105.6°C and 358.7°C; 2) better reliability in evaluating battery safety properties, given that all of the 4 tested batteries in the Aluminum-Anode ISCr experiment yield the consistent explosion behavior while the nail penetration test doesn't have explosion. It is convenient to implant the proposed SMA ISCr trigger into batteries for ISCr experiments and safety evaluation. Besides, it is also effective to use this method to verify battery fault detection methods, establish battery ISCr/safety simulation models and improve our understanding of battery ISCr problem, which will further benefit the safety design of battery and battery management system.

Acknowledgment

This work is supported by the National Natural Science Foundation of China under the grant No. U1564205 and funded by the Ministry of Science and Technology of China under the grant No. 2016YFE0102200. The first author is funded by China Scholarship Council. The author thank the participation in the experiments of Guohua Li, Chunyan Guo, Jianxun Ren, Qing Liu from Jiangsu Huadong Institute of Li-ion Battery, and Fang Wang, Bin Fan, Hongqing Wang from CATARC.

References

1. Y. Zheng, M. Ouyang, L. Lu, and J. Li, "Understanding aging mechanisms in lithium-ion battery packs: From cell capacity loss to pack capacity evolution," *J. Power Sources*, **278**, 287 (2015).
2. H. Maleki and J. N. Howard, "Internal short circuit in Li-ion cells," *J. Power Sources*, **191**, 568 (2009).
3. N. A. Chaturvedi, R. Klein, J. Christensen, J. Ahmed, and A. Kojic, "Algorithms for advanced battery-management systems," *IEEE Control System*, **30**, 49 (2010).
4. S. Santhanagopalan, P. Ramadass, and J. Zhang, "Analysis of internal short-circuit in a lithium ion cell," *J. Power Sources*, **194**, 550 (2009).
5. E. Sahraei, J. Campbell, and T. Wierzbicki, "Modeling and short circuit detection of 18650 Li-ion cells under mechanical abuse conditions," *J. Power Sources*, **220**, 360 (2012).
6. X. Feng, M. Fang, X. He, M. Ouyang, L. Lu, H. Wang, and M. Zhang, "Thermal runaway features of large format prismatic lithium ion battery using extended volume accelerating rate calorimetry," *J. Power Sources*, **255**, 294 (2014).
7. A. Jana, Da. R. Ely, and R. E. Garcia, "Dendrite-separator interactions in lithium-based batteries," *J. Power Sources*, **275**, 912 (2015).
8. P. Ramadass, W. Fang, and Z. Zhang, "Study of internal short in a Li-ion cell I. Test method development using infra-red imaging technique," *J. Power Sources*, **248**, 769 (2014).
9. J. Jeevarajan, *Determination of Tolerance to Internal Shorts and Its Screening in Li-Ion Cells - NASA JSC Method*, NASA Aerospace Battery Workshop, Huntsville, AL, 2008.
10. J. T. Chapin and A. Wu, *Blunt Nail Crush Internal Short Circuit Lithium-ion Cell Test Method*, NASA Aerospace Battery Workshop, Huntsville, AL, 2009.
11. H. P. Jones, J. T. Chapin, and M. Tabaddor, Critical Review of Commercial Secondary Lithium-Ion Battery Safety Standards, Proceedings of the fourth IAASS Conference: Making Safety Matter, Huntsville, AL, 2010.
12. J. Lamb and C. J. Orendorff, "Evaluation of mechanical abuse techniques in lithium ion batteries," *J. Power Sources*, **247**, 189 (2014).
13. W. Cai, H. Wang, H. Maleki, J. Howard, and E. Lara-Curzio, "Experimental simulation of internal short circuit in Li-ion and Li-ion-polymer cells," *J. Power Sources*, **196**, 7779 (2011).
14. C. J. Orendorff, P. Roth, C. Carmignani, J. Langendorf, and L. Davis, *External Triggers for Internal Short Circuits in Lithium Ion Batteries*, 215th ECS Meeting, San Francisco, CA, 2009.
15. C. J. Orendorff, P. Roth, and T. Lambert, *Lithium-Ion Cell Safety Issues of Separators and Internal Short Circuits*, 218th ECS Meeting, Las Vegas, NV, 2010.
16. C. J. Orendorff, E. P. Roth, and G. Nagasubramanian, "Experimental triggers for internal short circuits in lithium-ion cells," *J. Power Sources*, **196**, 6554 (2011).
17. C. McCoy, M. Menard, M. C. Laupheimer, D. Ofer, B. Barnett, and S. Sriramulu, *Implantation, Activation, Characterization and Prevention/Mitigation of Internal Short Circuits in Lithium-Ion Cells*, DOE Annual Merit Review Meeting, 2012.
18. M. Keyser, D. Long, Y. S. Jung, and A. Pesaran, *Development of a Novel Test Method for On-Demand Internal Short Circuit in a Li-Ion Cell*, Advanced Automotive Battery Conference, Pasadena, CA, 2011.
19. G. Kim, M. Keyser, and A. Pesaran, *DOE Vehicle Technologies Program Review*, Project ID: ES109, 2011.
20. IEEE 1625 *IEEE Standard for Rechargeable Batteries for Multi-cell Mobile Computing Devices*, 2008.
21. W. Fang, P. Ramadass, and Z. Zhang, "Study of internal short in a Li-ion cell-II. Numerical investigation using a 3D electrochemical-thermal model," *J. Power Sources*, **248**, 1090 (2014).
22. L. M. Schetky, 2000. *Shape-Memory Alloys*. Kirk-Othmer Encyclopedia of Chemical Technology.
23. D. Hwang and T. Higuchi, "A rotary actuator using shape memory alloy (SMA) wires," *IEEE/ASME Transactions on Mechatronics*, **19**, 1625 (2014).
24. D. Hwang and T. Higuchi, "A planar wobble motor with a XY compliant mechanism driven by shape memory alloy," *IEEE/ASME Transactions on Mechatronics*, **21**, 302 (2016).
25. A. B. Hegana, S. I. Hariharan, and E. D. Engeberg, "Electromechanical conversion of low-temperature waste heat via helical shape memory alloy actuators," *IEEE/ASME Transactions on Mechatronics*, **21**, 1434 (2016).
26. M. Ouyang, M. Zhang, X. Feng, L. Lu, J. Li, X. He, and Y. Zheng, "Internal short circuit detection for battery pack using equivalent parameter and consistency method," *J. Power Sources*, **294**, 272 (2015).